https://doi.org/10.20965/jdr.2021.p0561

Paper:

Real-Time Slope Stability Analysis Utilizing High-Resolution Gridded Precipitation Datasets Based on Spatial Interpolation of Measurements at Scattered Weather Station

Nanaha Kitamura[*1,†], Akino Watanabe[*1], Akihiko Wakai[*1], Takatsugu Ozaki[*1], Go Sato[*2], Takashi Kimura[*3], Jessada Karnjana[*4], Kanokvate Tungpimolrut[*4], Seksun Sartsatit[*4], and Udom Lewlomphaisarl[*4]

[*1]Gunma University
1-5-1 Tenjin-cho, Kiryu, Gunma 376-8515, Japan
[†]Corresponding author, E-mail: t180c031@gunma-u.ac.jp
[*2]Teikyo Heisei University, Tokyo, Japan
[*3]Ehime University, Ehime, Japan
[*4]National Electronics and Computer Technology Center, Pathum Thani, Thailand
[Received December 5, 2020; accepted February 22, 2021]

Measuring the amount of rainfall is essential for a wide-area evaluation of the risk of landslide disaster using a real-time simulation. In Thailand, located in Monsoon Asia, point observation is conducted using a rain gauge. Interpolation calculation is crucial for obtaining the planar rainfall intensity for the wide-area analysis from scattered point observation data. In this study, to accurately calculate rainfall intensity using the inverse distance weighting (IDW) method, the parameters affecting the results are examined. Additionally, using obtained rainfall data, a simple prediction calculation of groundwater level fluctuation by Wakai et al. [1] and Ozaki et al. [2] is performed. Finally, the relationship between the rainfall intensity and the fluctuation of groundwater level will be discussed.

Keywords: numerical simulation, inverse distance weighting method, rainfall data, slope failure, groundwater level

1. Introduction

Recently, the extreme weather conditions caused by global climate change have resulted in an escalation of landslide disasters. To address this, many proposals have been put forth based on the short-time calculation of real-time evaluation of landslide disaster risk (for example, Misumi et al. [3], Okimura et al. [4], Kinoshita et al. [5]). Wakai et al. [1] and Ozaki et al. [6] have proposed simplified prediction models of groundwater level fluctuation based on the finite element method. For performing the numerical analysis, it is necessary to input rainfall data to all points in a spatially discretized grid shape and observe the input value. In Japan, country-wide high-performance X-Band MP radars are deployed, and wide-area and high-density rainfall observation is conducted (Kuran [7]). However, in Monsoon Asia, where landslide disasters occur and radar analysis networks similar to those in Japan are not in place, point observations using rain gauges are performed. However, it is important to obtain a wide-area rainfall intensity to evaluate the risk of landslide disasters in Thailand and Vietnam, which are also located in Monsoon Asia. In this study, prediction by interpolation calculation to measure wide-area rainfall intensity from rainfall data obtained by a point observation using a rain gauge is conducted (**Fig. 1**).

This study conducts an analysis in Chiang Mai in northern Thailand to accurately predict the rainfall intensity. Next, the rainfall intensity obtained by interpolation calculation is applied to the method proposed by Wakai et al. [1] and Ozaki et al. [2] to conduct a simple prediction calculation of groundwater level fluctuation. Finally, the results of the analysis will be discussed, and a method to obtain the wide-area rainfall intensity necessary for landslide disaster risk evaluation will be proposed.

2. Rainfall Interpolation Calculation Using Inverse Distance Weighting (IDW) Method

2.1. Outline of IDW Method

As a simple interpolation calculation method for predicting the planar rainfall intensity from the rainfall data obtained by point observation, examinations have been conducted using the inverse distance weighting (IDW) method (Chen and Liu [8]), kriging (Goovaerts [9]), spline (Hutchinson [10]), and so on. For a real-time evaluation of slope failure risk in heavy rain, it is essential to use a method with a small calculation load that immediately provides a solution. Therefore, this study uses the IDW method described by Li and Heap [11] (**Fig. 2**).

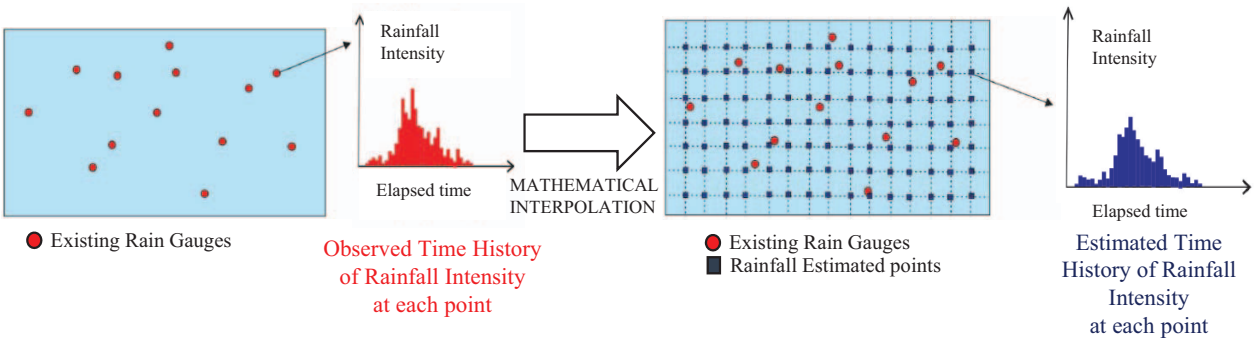

Fig. 1. Interpolation calculation of rainfall.

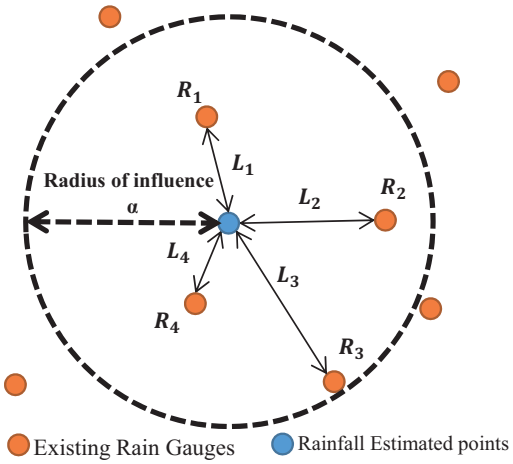

Fig. 2. Conceptual view of IDW method.

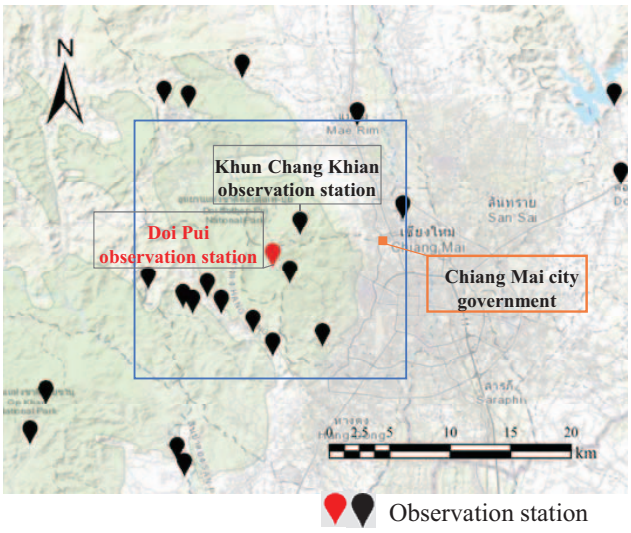

Fig. 3. Locations of observation stations around Doi Pui Village.

The IDW method's calculation formula is expressed by the following equations, where R is the rainfall at the interpolation point, R_i is the known rainfall observation data, L_i is the distance from the interpolation point (alternatively, the distance on the coordinate system obtained from the latitude and longitude), P_i is the weight of the inverse distance, k is the multiplier of the weight of the inverse distance, and n is the number of observation data.

$$P_i = \frac{1}{L_i^k}, \quad \ldots\ldots\ldots\ldots\ldots\ldots\ldots\ldots\ldots\ldots (1)$$

$$R = \frac{\sum_{i=1}^{n} P_i R_i}{\sum_{i=1}^{n} P_i}. \quad \ldots\ldots\ldots\ldots\ldots\ldots\ldots\ldots\ldots\ldots (2)$$

In this method, the smaller the distance of interpolation points, the larger the effect of the point on the interpolation value. That is, the superiority of the known point observation data for the interpolation value can be controlled by the multiplier k of the weight; the larger the k, the higher the superiority of a near point, and the lower the superiority of a distant point. Here, it is necessary to determine the range of observation data, which is the target of the calculation of interpolation point. For this, the radius of influence α [km] from a discretionary point is determined, and the points within the radius of influence are included in the calculation.

2.2. Input Conditions Used in IDW Method and its Application to Target Sites

In this study, the IDW method is used to apply for the analysis around Doi Pui Village of Chiang Mai. This method uses the rainfall data provided by the Department of Disaster Prevention and Mitigation (DDPM) of Thailand. **Fig. 3** shows the locations of the observation stations around and rain gauge at Doi Pui Village (hereinafter referred to as the Doi Pui observation station). The validity of calculation results by the IDW method is examined by estimating the rainfall – regardless of the observation data – and comparing the estimated rainfall with the actual measurement value of the Doi Pui observation station. The collection interval of the actual measurement value by the rain gauge is five minutes. The 24 hours rainfall data were used that were observed at the Doi Pui observation station on August 21, which recorded the highest rainfall in August 2019.

As input conditions of the IDW method, the inverse

Table 1. Examination items of input conditions of IDW method.

Inverse distance weight multiplier k	1, 2, 3, 4, 5
Radius of influence α [km]	3.5–30

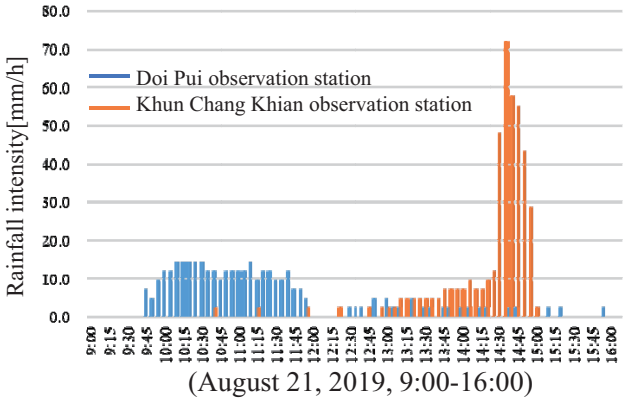

Fig. 4. Rainfall intensity at Doi Pui observation station and Khun Chang Khian observation station.

distance weight multiplier k and the radius of influence α [km] are determined by calculating the result under the conditions of $k = 1, 2, 3, 4, 5$, $\alpha = 3.5$ to 30 km (**Table 1**). The root mean squared error (RMSE) was used for examining the validity of the result.

The groundwater level rises after rainwater infiltration and storage in the ground during rainfall (Wakai et al. [1], Ozaki et al. [2]). The accumulative amount of rainfall over time and the temporary rainfall intensity affect the evaluation of landslide disaster risk by predicting the groundwater level fluctuation. Due to the movement of rain clouds, rainfall in the observation point of the target area is sometimes accompanied by a time delay depending on the spatial arrangement. For example, **Fig. 4** shows the rainfall intensity observed at the Doi Pui observation station and the Khun Chang Khian observation station (**Fig. 3**). The rainfall intensity was high in Doi Pui Village from around 9:45 to around 11:45, while the rainfall intensity was low at the Khun Chang Khian observation station. However, the rainfall intensity was high at the Khun Chang Khian observation station from around 13 o'clock to around 15 o'clock. Such a phenomenon also occurred at other observation stations. Therefore, based on the spatial distribution of rainfall over time, the rainfall intensity is evaluated focusing on the accuracy of the accumulative rainfall data and the prediction of the observed rainfall at 5-minute intervals. We calculate and evaluate accumulative rainfall for 1, 2, 3, 4, and 6 hours.

2.3. Accuracy Evaluation Method Using RMSE

To decide the input conditions necessary for applying the IDW method around Doi Pui Village, the accuracy is evaluated using the RMSE described by Phogat et al. [12]. The calculation formula is expressed by Eq. (3), where M_i is the actual measurement value at the Doi Pui observation station, S_i is the prediction value calculated by IDW method, and N is the number of data.

$$\mathrm{RMSE} = \sqrt{\frac{1}{N}\sum_{i=1}^{N}(M_i - S_i)^2}. \quad \ldots\ldots\ldots \quad (3)$$

RMSE indicates that the smaller the calculated value, the smaller the difference between the actual measurement value and the prediction value, and the higher the accuracy of the prediction value. The value obtained by Eq. (3) is in the same unit as that in the rainfall data. RMSE for the accumulative rainfall of 1 hour to 6 hours is calculated in addition to the rainfall of the 5-minute intervals, and all units are unified by converting them into [mm/h].

2.4. Examination of Inverse Distance Weight Multiplier k

The inverse distance weight multiplier k in Eq. (1) changes the effect of observation data on the interpolation points when the IDW method is used. Section 2.4 examines the setting of this parameter. The amount of rainfall at the Doi Pui observation station is estimated by conducting an interpolation calculation from the observed amount of rainfall at the Doi Pui observation station, except for the actual measurement amount at the observation station. At this point, the rainfall amount is calculated by varying k from 1 to 5 in the rainfall data observed on August 21 and these values are compared it with the actual measurement value. The calculation is performed with the radius of influence assumed to be about 14 km from the Doi Pui observation station, where the data are relatively concentrated. As mentioned above, the examination and evaluation are accumulatively carried out, in addition to the rainfall data observed at 5-minute intervals.

Figure 5 shows the result of the interpolation calculation of the rainfall intensity on the 1 km grid at $k = 1$ to 5 in the range surrounded by the blue line of about 20 km × 20 km including the Doi Pui observation station in **Fig. 3**. The results at 10 o'clock on August 21, 2019, are shown. **Fig. 5** shows that the effect of the observation data near the interpolation point becomes larger by increasing k.

Figure 6 shows the actual observation values at the Doi Pui observation station and the accumulative values of the rainfall data interpolated by varying k from 1 to 5. The case of $k = 2$ is most similar to the actual observation value at the Doi Pui observation station. Therefore, **Fig. 6** also shows prediction and observation values of rainfall intensity observed every five minutes with $k = 2$. Comparison of the time series data indicates a difference in the results. Here, **Table 2** shows RMSE calculated from the actual observation value and prediction value at the Doi Pui observation station under the condition $k = 1$ to 5. In addition to the 5-minute interval observation values, the rainfall amounts of 1- to 6-hour accumulation were also compared. Comparison with the 5-minute interval data indicates that RMSE was the smallest when $k = 1$. Contrarily, RMSE was the smallest when $k = 2$ with a longer accumulation time. When using this value

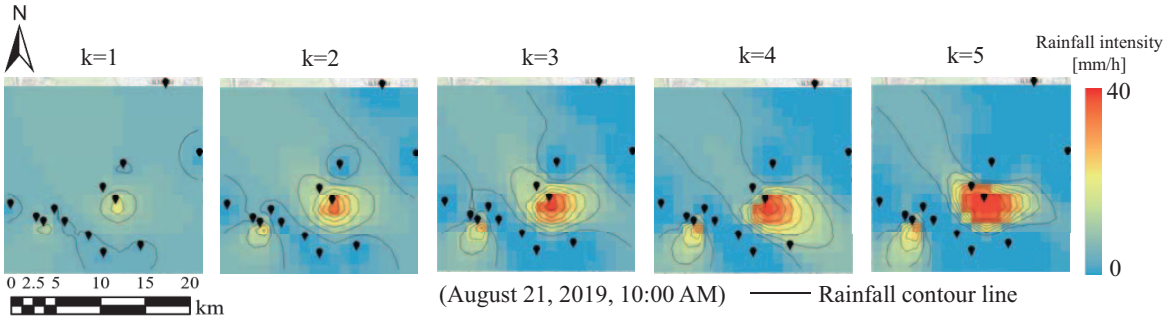

Fig. 5. Distribution of rainfall intensity by interpolation calculation with multiplier k being varied in range shown in blue (**Fig. 3**).

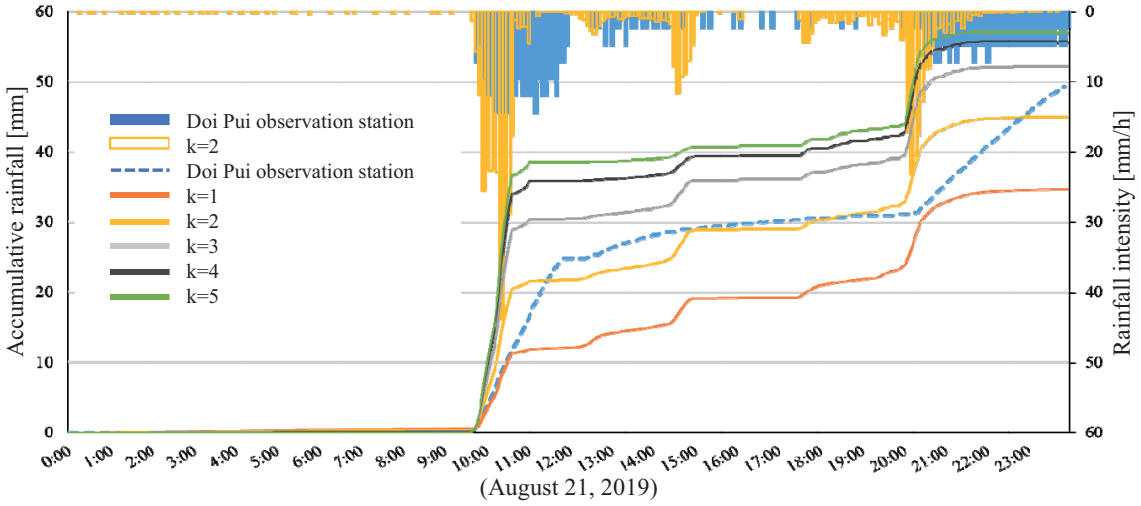

Fig. 6. Comparison of observation values at Doi Pui observation station with accumulative values of rainfall data interpolated by varying k from 1 to 5, and comparison of observation values and prediction values of rainfall intensity every five minutes when $k = 2$.

Table 2. RMSE calculated from actual observation values and prediction values at Doi Pui observation station under condition of $k = 1$ to 5.

Rainfall data used for RMSE (Actual measurement values and prediction values)	RMSE [mm/h] Points in yellow indicate the minimum values of each rainfall				
	k=1	k=2	k=3	k=4	k=5
5-minute interval data	3.73	4.67	6.13	7.16	7.72
1-hour accumulative rainfall	2.85	3.00	3.73	4.34	4.69
2-hour accumulative rainfall	2.32	1.68	1.59	1.82	2.01
3-hour accumulative rainfall	2.35	1.90	2.04	2.37	2.60
4-hour accumulative rainfall	1.59	0.80	0.84	1.27	1.55
6-hour accumulative rainfall	1.19	0.49	0.57	0.97	1.21

for response analysis of groundwater level, it is necessary to focus more on the accumulative rainfall that infiltrates into the ground than on the temporary rainfall. Therefore, the rainfall interpolation calculation was performed by adopting $k = 2$, which gave the best accuracy based on the accumulative rainfall.

2.5. Examination of Radius of Influence α [km]

The optimum value of the radius of influence is examined to decide the adoption of the point observation data. The radius of influence is varied around the Doi Pui observation station to increase the number of observation points, and the obtained values are evaluated using RMSE. As in Section 2.4, we used the rainfall data observed on August 21, 2019 and the inverse distance weight multiplier of $k = 2$ were used.

Table 3 shows the radius of influence used in the calculation, the number of observation points within the radius of influence, the results of evaluations by RMSE on the prediction values using these conditions, and the ac-

Table 3. RMSE calculated by the number of observation points and each rainfall amount when the radius of influence α [km] was varied.

Radius of influence	Number of observation points	RMSE [mm/h] Points in yellow indicate the minimum values of each rainfall					
α[km]	n	5-minute interval data	1-hour accumulative rainfall	2-hour accumulative rainfall	3-hour accumulative rainfall	4-hour accumulative rainfall	6-hour accumulative rainfall
3.5	2	6.50	4.04	1.82	2.18	0.97	0.70
6	5	5.27	3.31	1.60	1.88	0.69	0.44
7.5	7	5.08	3.21	1.63	1.90	0.69	0.42
8	9	4.85	3.10	1.67	1.92	0.73	0.43
11	11	4.71	3.02	1.68	1.91	0.78	0.47
15	13	4.63	2.98	1.68	1.90	0.81	0.49
19	17	4.54	2.93	1.70	1.89	0.85	0.53
25	19	4.51	2.92	1.69	1.89	0.85	0.53
30	21	4.49	2.91	1.69	1.89	0.86	0.54

tual measurement values of the Doi Pui observation station. The variation in RMSE indicates that in the case of accumulative rainfall, RMSE was significantly reduced at about 3.5 to 8 km radius of influence and 2 to 9 observation points, and the change was small, on and after 11 km of the radius of influence and 10 observation points. When the accumulation time was made longer, the RMSE became the smallest while using the radius of influence of $\alpha = 7.5$ km. From the above results, the radius of influence of $\alpha = 7.5$ km became optimum when predicting rainfall using the IDW method by targeting the rainfall on August 21, 2019.

2.6. Confirmation of Rainfall Prediction Accuracy of the Condition Used for IDW Method at Doi Pui Observation Station

Until Section 2.5, the method of deciding – by RMSE – the necessary conditions for predicting the rainfall amount for the Doi Pui observation station using the IDW method have been examined. Consequently, the optimum conditions of the IDW method on August 21, 2019, were as follows: the inverse distance weight multiplier $k = 2$, the radius of influence $\alpha = 7.5$ km, and the number of observation points $n = 7$ in the radius of influence. To examine whether these conditions are applicable to other rainfall data, the rainfall under the same conditions were predicted using the IDW method, targeting the rainfall that occurred at the Doi Pui observation station in August 2019.

Figure 7 shows the results of the comparison between the actual measurement values and the accumulative rainfall predicted by the IDW method for the six cases in August 2019. The results obtained by the IDW method have successfully reproduced the actual measurement values with good accuracy for the other four days, except for cases 2 and 6. However, these cases were low in their accuracy of predicting the actual measurement values because there was a shortage in the observed rainfall at the seven points used in the IDW method compared with the observed rainfall at the Doi Pui observation station.

3. Calculation of Groundwater Level Fluctuation Using Interpolation Calculation Results

In Section 2, the multiplier k of the weight and the radius of influence α were examined in order to use the IDW method. In Section 3, the groundwater level fluctuation is calculated using the interpolated rainfall data based on these conditions.

3.1. Simple Prediction Model of Groundwater Level Fluctuation

The amount of groundwater level fluctuation in the shallow part in a natural slope is calculated assuming a single geological composition. The fluctuation amount is decided by the following models: the vertical infiltration through the ground surface and the lateral infiltration of groundwater level in the saturated zone.

3.1.1. Modeling of Vertical Infiltration Flow

Based on the saturated–unsaturated groundwater analysis (FEM program: VGFLOW (Cai and Ugai [13])), Wakai et al. [1] and Ozaki et al. [2] have built simplified prediction models of vertical infiltration capable of obtaining the amount of raised groundwater level with the same accuracy as FEM and in a short period. **Fig. 8** shows an example of the time history of the groundwater level and the saturation degree of an unsaturated layer during constant rainfall on a semi-infinite slope obtained by the finite element method. The groundwater level tends to elevate slightly until the saturation degree in the unsaturated layer reaches a certain level, even after the onset of rainfall. It tends to maintain an almost constant rate

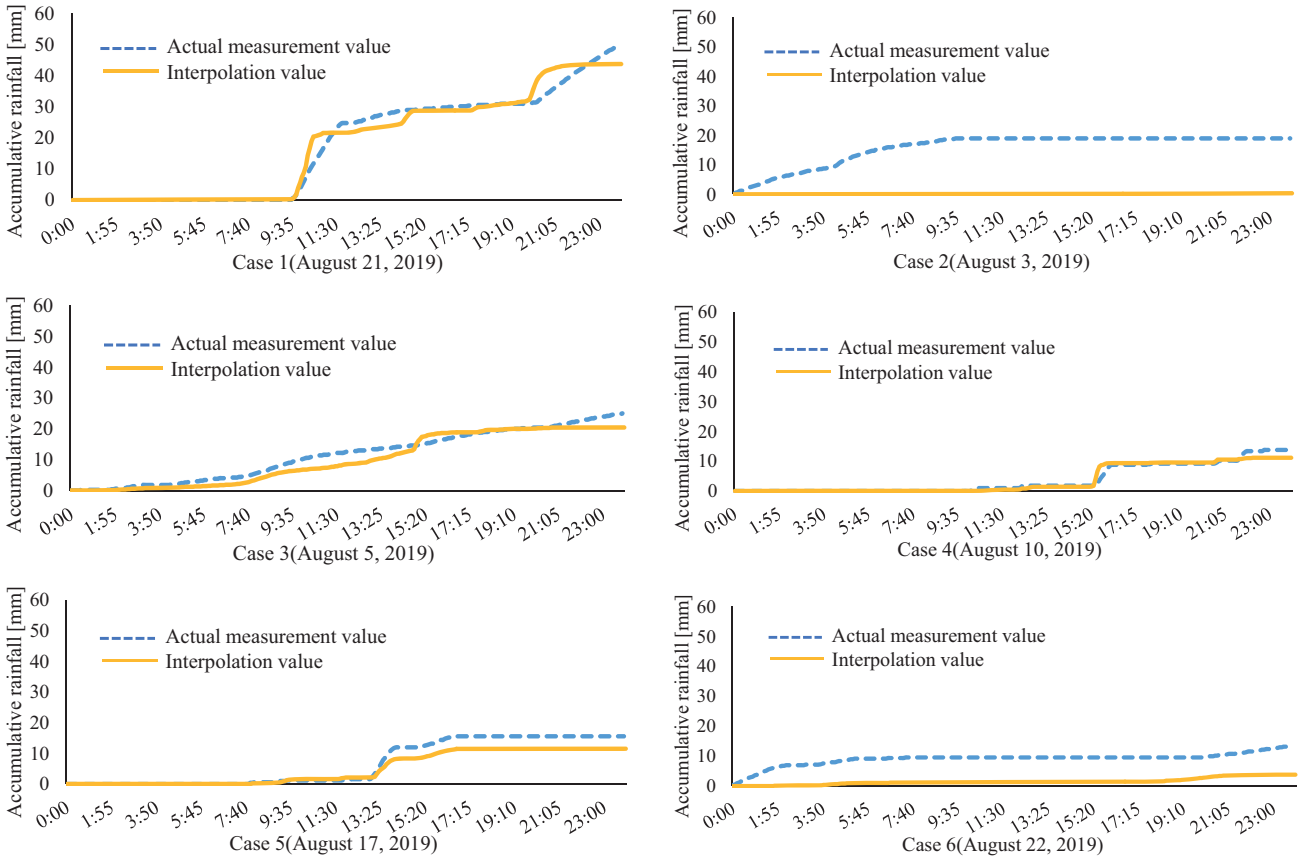

Fig. 7. Results of observation rainfall and accumulative rainfall calculated using IDW method ($k = 2$, $\alpha = 7.5$ km).

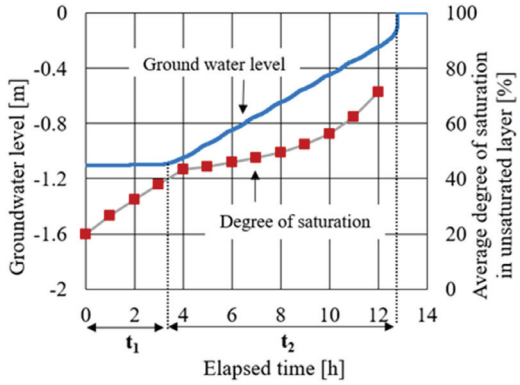

Fig. 8. Time histories of ground water level and degree of saturation.

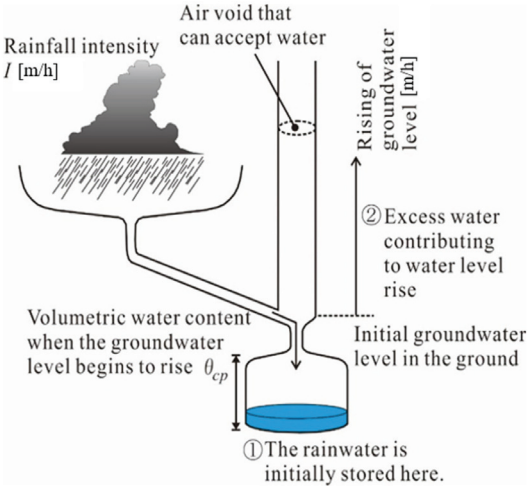

Fig. 9. Concept of the developed model for vertical infiltration in the slope.

of elevation, post-onset of elevation. Focusing on these two time zones, Wakai et al. [1] and Ozaki et al. [2] conducted modeling of vertical infiltration (**Fig. 9**). While assuming a constant rainfall intensity of I [m/h], assuming that all the rainwater has infiltrated into the ground, the elapsed time t_1 [h] until the water level rises is expressed by Eq. (4), where the soil porosity is n, the depth of the groundwater level before the onset of rainfall is h [m], and the initial saturation degree is S_{r0} [%].

$$t_1 = \frac{h}{I}\left(\theta_{cp} - n\frac{S_{r0}}{100}\right). \quad \cdots\cdots\cdots \quad (4)$$

In Eq. (4), θ_{cp} is the volumetric water content of upper limit at which the rainwater can stay in the ground (not contributing to the water level elevation), after infiltrating into an unsaturated layer. The elevation speed v_{wl} (however, the value obtained by multiplying the correction factor α_v of the speed) is obtained as a speed at which the saturated zone expands upward by filling the underground gap with water, post-onset of the water level elevation,

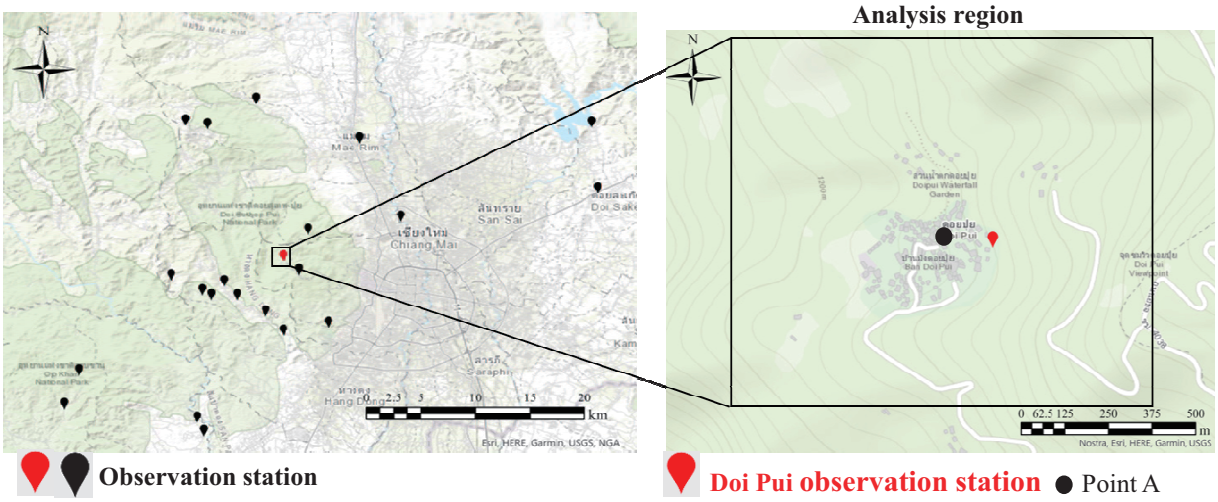

Fig. 10. Observation station locations and groundwater level analysis region.

after obtaining t_1. Assuming that the saturation degree when the elevation of the groundwater level starts is S_r^*, the elapsed time t_2 until the water level reaches the ground surface post-onset of water level elevation is obtained by Eq. (5).

$$t_2 = \frac{h}{v_{wl}} = \frac{n\left(1 - \frac{S_r^*}{100}\right)h}{\alpha_v I} \quad \ldots\ldots\ldots\ldots \quad (5)$$

Wakai et al. [1] and Ozaki et al. [2] have reported that simple phenomenon prediction is possible by back calculating from t_1 and t_2 obtained by a series of analyses and by determining, for each condition, the values of two parameters (θ_{cp} and α_v) that can cope with various conditions. The calculation results indicate that the θ_{cp} parameter differs depending on the inclination angle. It should be noted that α_v is constant ($= 2.1$) regardless of the conditions.

By applying the above-described Eqs. (4) and (5) – proposed by Wakai et al. [1] and Ozaki et al. [2], to actual rainfall – the fluctuation amount of the groundwater level due to vertical infiltration is calculated.

3.1.2. Modeling of Lateral Infiltration Flow

The planar flow in an unconfined aquifer, that is, the flow of groundwater along the aquifer, is given by the following governing equation (Japanese Association of Groundwater Hydrology [14]).

$$\frac{\partial}{\partial x}\left(T_{xx}\frac{\partial \Phi}{\partial x}\right) + \frac{\partial}{\partial y}\left(T_{yy}\frac{\partial \Phi}{\partial y}\right) = n_e \frac{\partial \Phi}{\partial t}, \quad \ldots \quad (6)$$

where T_{xx} and T_{yy} are the transmissibility coefficient (m^2/h), which is obtained by multiplying the hydraulic conductivity K [m/h] by the aquifer thickness (m), n_e represents the effective porosity, and Φ represents the total head (m). To obtain an immediate and comprehensive solution, instead of a large-scale matrix calculation, a method with a small calculation load is required.

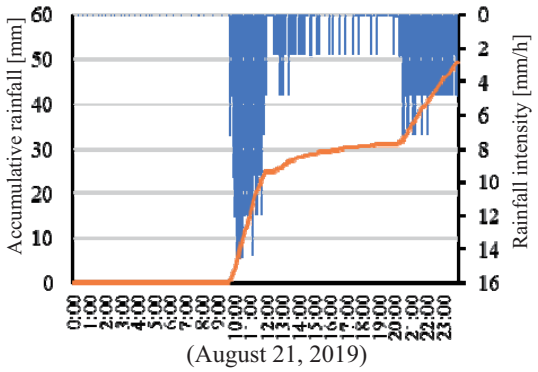

Fig. 11. Rainfall intensity at analysis region center (Point A).

Therefore, this method conducts a spatial and temporal approximation in accordance with the difference calculation algorithm of Kinzelbach [15] and numerically solves using an explicit method. The behavior of groundwater spread across a wide area due to rainfall is reproduced by calculating the vertical infiltration and lateral infiltration flow in a rectangular grid at regular intervals for each time difference.

3.2. Calculation of Groundwater Level Fluctuation in Doi Pui Village

3.2.1. Input Data

The analysis is carried out in a region of 1210 m × 1060 m including Doi Pui Village (**Fig. 10**). The calculation was performed by resampling DEM of 1-m resolution of AW3D to 5-m resolution by the nearest neighbor method, with the spatial difference of 5-m grid. The rainfall data are entered by interpolating the rainfall data of August 21, 2019, observed by DDPM of Thailand. The conditions of the IDW method are the previously-mentioned inverse distance weight multiplier of $k = 2$ and the radius of influence $\alpha = 7.5$ km, which are used for the interpolation points of the entire region. **Fig. 11** shows the

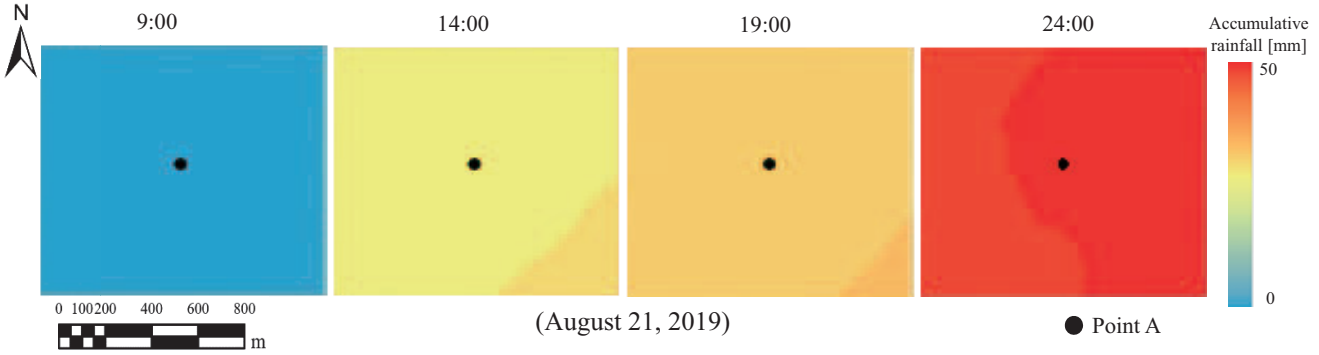

Fig. 12. Accumulative rainfall from 0:00 at each time point in target region.

Table 4. Parameters used in calculating groundwater level.

Medium sand	
Saturated hydraulic conductivity k [m/s]	10^{-4}
Porosity n	0.3
Initial unsaturated layer thickness (base depth) h [m]	2.0
Initial saturation degree S_{r0} [%]	60

time history of the rainfall intensity calculated at the center (Point A) of the target region. **Fig. 12** shows the accumulative rainfall at the stages of 9, 14, 19, and 24 o'clock. **Table 4** shows typical values of medium sand, regarding the parameters used for calculating groundwater level fluctuation, such as hydraulic conductivity. Assuming that the initial groundwater table is located below the bedrock surface, the thickness of the initial unsaturated layer, that is, the depth to the bedrock surface was set to 2 m this time, and the initial saturation degree was set at 60%.

3.2.2. Analysis Results of Groundwater Level in Doi Pui Village

Figure 13 shows the groundwater level at the stages of 9, 14, 19, and 24 o'clock as in the accumulative rainfall shown in **Fig. 12**. The accumulative rainfall reached 49 mm up to 24 o'clock after the onset of the rainfall. At this time, the groundwater level increased with the increase in the accumulative rainfall, and it was elevated from −2 m (GL-m) of the groundwater level at the time of initiating the analysis to −1.87 (GL-m) near the ground surface at Point A, for example. The fluctuation and relevance of rainfall and groundwater level can play important roles when conducting future simulation analysis. In this regard, the results calculated by the analysis method used in this study can be adopted as a basic condition of future simulation analysis. Thus, the rainfall interpolation calculation using the IDW method can be beneficial in conducting the response calculation of groundwater level over a wide area.

4. Conclusions

In this paper, the analysis was conducted using the IDW method as one of the methods of calculating the planar rainfall intensity from the rainfall data obtained by point observation around Doi Pui Village in Chiang Mai, Thailand. When using the IDW method, it is essential to decide the inverse distance weight multiplier k and the radius of influence α. In this study, those conditions were decided using RMSE. Since comparison of the actual measurement values at the Doi Pui observation station with the results predicted by the IDW method, the condition of the IDW method was decided as the one providing the best accuracy when predicting a single point. During the application of the IDW method in a different location from that in this study, there is a possibility that the optimum condition is different depending on the arrangement of rain gauges and the tendency of rainfall. Hence, it is necessary to decide the inverse distance weight multiplier and the radius of influence based on the target region. When using the conditions of the IDW method decided at the Doi Pui observation station for the groundwater level fluctuation calculation of Wakai et al. [1] and Ozaki et al. [2], the rainfall data were entered and the values for the entire target region were calculated. Additionally, the planar groundwater level for over time was calculated. Consequently, the relation between the increase in the accumulative rainfall and the elevation tendency of the groundwater level was suggested. In the future, conducting the risk assessment of landslide disaster in a wide area in Monsoon Asia may be an issue, particularly by combining such a method with the rainfall interpolation calculation.

Acknowledgements

Part of this work was supported by JST SICORP (e-ASIA Joint Research Program) Grant Number JPMJSC18E3, Japan. The authors wish to acknowledge Mr. Komson Suwanampha, the vice governor of Chiang Mai Provincial Governer Office, and Department of Disaster Prevention and Mitigation (DDPM), Ministry of Interior, Thailand, who has helped us in our collaborative efforts on slope disaster prevention in Thailand.

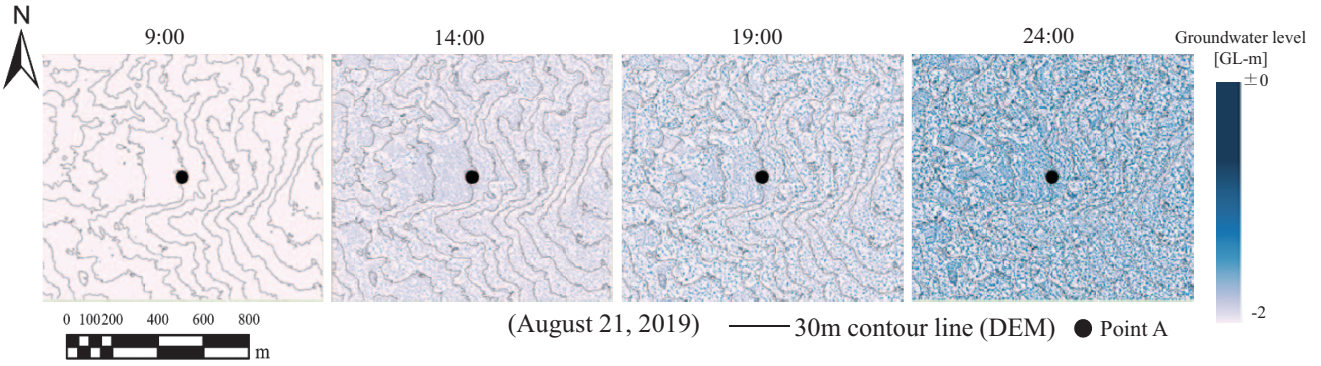

Fig. 13. Groundwater level at each time point in target region.

References:

[1] A. Wakai, K. Hori, A. Watanabe, F. Cai, H. Fukazu, S. Goto, and T. Kimura, "A simple prediction model for shallow groundwater level rise in natural slopes based on finite element solutions," J. of the Japan Landslide Society, Vol.56, No.Special_Issue, pp. 227-239, 2019 (in Japanese).

[2] T. Ozaki, A. Watanabe, A. Wakai, and F. Cai, "A Simple Prediction Model for Shallow Groundwater Level Rising in Natural Slopes Based on Finite Element Analysis," Geotechnics for Sustainable Infrastructure Development, pp. 993-1000, 2019.

[3] R. Misumi, T. Oguchi, M. Maki, and K. Iwanami, "A real-time forecast of shallow landslides using a distributed rainfall-runoff model," Japan Society for Natural Disaster Science, Vol.23, No.3, pp. 415-432, 2004 (in Japanese).

[4] T. Okimura, N. Torii, Y. Osaki, M. Nambu, and K. Haraguchi, "Construction of real-time type hazard system to predict landslides caused by heavy rainfalls," J. of the Japan Society of Erosion Control Engineering, Vol.63, No.6, pp. 4-12, 2011 (in Japanese).

[5] A. Kinoshita, T. Kanno, A. Okamoto, M. Hitokoto, M. Onodera, M. Sakuraba, and M. Sugiyama, "Construction of real-time hazard map system in Rokko mountain area," J. of the Japan Society of Erosion Control Engineering, Vol.66, No.1, pp. 15-22, 2013 (in Japanese).

[6] T. Ozaki, A. Wakai, A. Watanabe, F. Cai, G. Sato, and T. Kimura, "A simplified model for the infiltration of rainwater in natural slope consisting of fine sands," J. of the Japan Landslide Society, Vol.58, No.2, pp. 57-64, 2021 (in Japanese).

[7] S. Kuran, "X-Band Polarimetric (Multi Parameter) Radar for Heavy Rainfall Disaster," The J. of the Institute of Electrical Installation Engineers of Japan, Vol.34, No.3, pp. 180-183, 2014 (in Japanese).

[8] F.-W. Chen and C.-W. Liu, "Estimation of the spatial rainfall distribution using inverse distance weighting (IDW) in the middle of Taiwan," Paddy and Water Environment, Vol.10, No.3, pp. 209-222, 2012.

[9] P. Goovaerts, "Geostatistical approaches for incorporating elevation into the spatial interpolation of rainfall," J. of Hydrology, Vol.228, Nos.1-2, pp. 113-129, 2000.

[10] M. F. Hutchinson, "Interpolating mean rainfall using thin plate smoothing splines," Int. J. Geographical Information Systems, Vol.9, No.4, pp. 385-403, 1995.

[11] J. Li and A. D. Heap, "A Review of Spatial Interpolation Methods for Environmental Scientists," Geoscience Australia, p. 137, 2008.

[12] V. Phogat, A. K. Yadav, R. S. Malik, S. Kumar, and J. Cox, "Simulation of salt and water movement and estimation of water productivity of rice crop irrigated with saline water," Paddy and Water Environment, Vol.8, pp. 333-346, 2010.

[13] F. Cai and K. Ugai, "Numerical Analysis of Rainfall Effects on Slope Stability," Int. J. of Geomechanics, Vol.4, No.2, pp. 69-78, 2004.

[14] Japanese Association of Groundwater Hydrology, "Simulation of ground water flow and solute transport," pp. 47-51, 2014 (in Japanese).

[15] W. Kinzelbach, "Groundwater modelling: An introduction with sample programs in BASIC," pp. 29-35, Elsevier Science Ltd, 1986.

Name:
Nanaha Kitamura

Affiliation:
Undergraduate Student, Geotechnical Engineering Laboratory, Department of Environmental Engineering Science, Gunma University

Address:
1-5-1 Tenjin-cho, Kiryu, Gunma 376-8515, Japan

Name:
Akino Watanabe

Affiliation:
Graduate Student, Geotechnical Engineering Laboratory, Department of Environmental Engineering Science, Gunma University

Address:
1-5-1 Tenjin-cho, Kiryu, Gunma 376-8515, Japan

Name:
Akihiko Wakai

Affiliation:
Professor, Gunma University

Address:
1-5-1 Tenjin-cho, Kiryu, Gunma 376-8515, Japan

Name:
Takatsugu Ozaki

Affiliation:
Ph.D. Student, Graduate School of Science and Technology, Gunma University
Address:
1-5-1 Tenjin-cho, Kiryu, Gunma 376-8515, Japan

Name:
Go Sato

Affiliation:
Professor, Graduate school of Environmental Informations, Teikyo Heisei University
Address:
4-21-2 Nakano, Tokyo 164-8530, Japan

Name:
Takashi Kimura

Affiliation:
Assistant Professor, Graduate School of Agriculture, Ehime University
Address:
3-5-7 Tarumi, Matsuyama, Ehime 790-8566, Japan

Name:
Jessada Karnjana

Affiliation:
National Electronics and Computer Technology Center
Address:
112 Thailand Science Park, Khlong Luang, Pathum Thani 12120, Thailand

Name:
Kanokvate Tungpimolrut

Affiliation:
Researcher, Advanced Control and Electronics Research Group, National Electronics and Computer Technology Center
Address:
112 Thailand Science Park, Pathum Thani, Thailand

Name:
Seksun Sartsatit

Affiliation:
National Electronics and Computer Technology Center
Address:
112 Thailand Science Park, Khlong Luang, Pathum Thani 12120, Thailand

Name:
Udom Lewlomphaisarl

Affiliation:
Senior Research Engineer, National Electronics and Computer Technology
Address:
112 Phahonyothin Road, Khlong Nueng, Khlong Luang District, Pathumthani 12120, Thailand